ANALYSIS AND MODELING OF THERMALLY INDUCED POSITIONING ERRORS BASED ON LASER INTERFEROMETER MEASUREMENTS

Salah AMROUNE[1], [2] and Mohamed SLAMANI, [2]
[1]*Department of Mechanical Engineering, Faculty of Technology, University of M'sila, Algeria.*
[2] *Materials and Structural Mechanics Laboratory (LMMS). University of M'sila. Algeria*
E-mail: salah.amroune@univ-msila.dz. mohamed.slamani@univ-msila.dz

ABSTRACT: *The accuracy of a machine tool can be significantly impacted by thermal deformation, which is a type of thermal error. Thermally induced positioning errors can occur due to temperature variations that cause the materials in a machine tool to expand or contract, leading to dimensional changes that affect the accuracy of position measurements. Laser interferometer measurements can be used to detect these errors by comparing the actual position of a component to its expected position based on a reference measurement. To control the thermally induced positioning error of machine tools, a mathematical model that describes the relationship between temperature and positioning errors is proposed in this paper. The proposed model is based on empirical data collected from laser interferometer measurements and then used to predict the magnitude of the errors under different thermal conditions. A set of tests was conducted to confirm the thermal model's validity. The excellent match between the experimental data and the calculated values provides evidence supporting the possibility of using the suggested approach for estimating the thermal performance of CNC machine tools.*

KEYWORDS: *Positioning error; thermal error; modeling; ,machine tool; laser interferometer.*

1 INTRODUCTION

Numerically controlled (CNC) machine tools have become indispensable in industrial manufacturing processes, particularly for their ability to produce high-precision, consistent quality parts. However, despite their efficiency, these machines are not perfect and can generate positioning errors that can affect the quality of the parts produced.

Positioning errors are caused by various factors such as geometric errors of machine components [1-3], thermal errors due to temperature fluctuations [4-6], deviation errors caused by cutting forces [7-9], machine axis servo errors [10], NC interpolation algorithmic errors and others [11-15]. Among them, thermal errors represent an important part ranging from 40 to 70% of the total errors.

Modeling positioning errors is an essential step to minimize these errors and ensure optimal precision in manufacturing processes. This modeling makes it possible to understand the sources of error and to correct them appropriately, which can contribute to improving the quality of the produced parts.

The main goal of this study is to investigate the thermally induced positioning errors of a CNC machine tool. Then, an analytical model for predicting the thermally induced positioning errors under different working conditions is proposed. The different sources of error and their impact on the precision of the machine, as well as the methods of modeling and correcting thermal errors were presented first. Then the advantages and limitations of these methods and their practical application in the manufacturing industry are discussed. Finally, concluded by emphasizing the importance of positioning error modeling to ensure consistent quality and increased efficiency in manufacturing processes.

2 MATERIALS AND METHODS

2.1 Material preparation

Achieving accurate estimates and effective machine tool error compensation requires the establishment of an empirical database that combines several critical parameters. Indeed, this database must include the commanded position of the machine tool, which corresponds to the target position of the axis and which is determined by the program being executed. In addition, the absolute position of the machine tool and the error associated with that position must be measured directly from a PC-controlled laser interferometer and stored in the

database. Finally, the thermal and environmental conditions under which the machine tool is tested must also be quantified and recorded using sensors installed on the machine.

Thus, the empirical database necessary for the estimation and compensation of machine tool errors must contain a large amount of accurate and reliable information. It must be able to take into account all the factors likely to affect the performance of the machine tool, in particular the environmental conditions (temperature, humidity, vibrations, etc.) as well as variations in the position of the axis. This database will then make it possible to effectively correct machine tool errors, improve the quality of manufactured products and reduce the costs associated with rework and lost production.

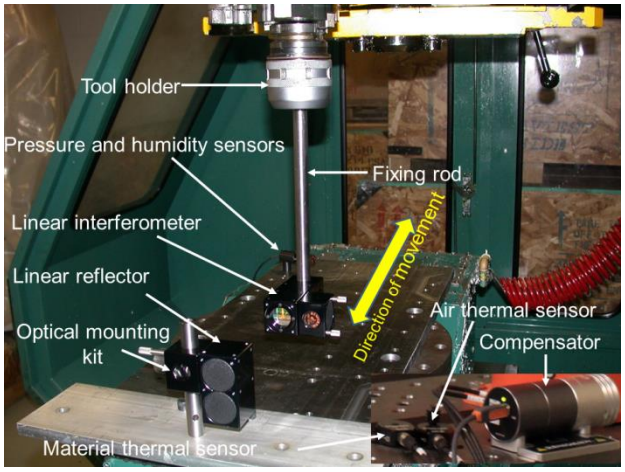

Fig.1 Laser interferometer setup for measuring linear position errors along the X-axis of the Matsuura MC.760 VX MOCN

2.2 Experimental procedure

Renishaw's laser measurement system is routinely used to perform all linear motion error measurements. The scene and the setup of the measurement with laser interferometer are shown in Fig. 1. The laser interferometer system in question is made up of a set of five main units that work in concert to ensure optimal operation. Each unit plays a specific role in the process and is essential to the overall performance of the system. The synergy between these key components achieves high quality results and ensures effective and efficient use of the system, it is composed of:

1. The ML10 laser head uses a low power (1mW) Class II HeNe laser beam with a nominal wavelength of 0.633mm (under vacuum) and long-term wavelength stability (under vacuum) 0.1ppm;
2. Renishaw linear optics kit including linear interferometer and retroreflector;
3. Environmental compensation unit for air temperature, air humidity, air pressure and material temperature measurements;
4. PC Gateway 2000 P166 installed with Renishaw laser measurement and data logging software;
5. PCMCIA interface card for data communication with PC Gateway 2000 P166 via data link cable.

A photo of mounting the Renishaw laser on the steel plate for testing along the X-axis of the Matsuura MC.760 VX MOCN and the placement locations of the temperature and pressure sensors are shown in (Figure 1). In addition to material temperature sensors, an air temperature sensor magnetically attached to the machine table as well as air pressure and humidity sensors were used to monitor environmental effects. Automatic environmental compensation uses the XC compensator to compensate for wavelength and thermal expansion of the material. If calibration is performed in an environment where atmospheric conditions are likely to vary during the test, automatic compensation is strongly recommended. The air and material temperature sensor used in this test is a smart sensor. Integrated microprocessors analyze and process sensor data before sending digital temperature values to the XC-80 compensator. More reliable measurements are thus obtained. It is also one of the main factors for the compactness of the XC-80. In addition, during this test, the atmospheric temperature sensor was placed as close as possible to the measurement line of the laser beam, without interfering with the measurement process and far from any localized heat sources such as motors or DC currents. The air temperature sensor was magnetically attached to the steel plate, next to it are the air pressure and humidity sensors to monitor environmental effects.

The system takes a reading every seven seconds from one of its environmental sensors, which is then transmitted to the computer. This reading is used to update the environment compensation factor. The environmental sensor readings are taken in a set order, i.e. air temperature, relative humidity, atmospheric pressure, followed by the three material thermal sensors.

2.3 Measurement procedure

For most machine tool calibration setups, it is recommended to mount the XL laser on the tripod and platform. The universal tripod and platform provide a stable mount for the XL laser that allows it to be positioned at different heights and provides complete alignment control of the laser beam.

As shown in Figure 1, the linear interferometer is positioned in the beam path between the Laser XL and the linear reflector. During linear measurements, one of the optical components

remains stationary while the other moves on the linear axis. In this test, the reflector is installed as a mobile optical component and the interferometer as a stationary component. When mounting the ML10, the laser beam is aligned to avoid dead path and cosine errors. Full beam strength was achieved over the entire axis travel during the measurements. After having a full signal strength, the measurement cycle was launched immediately (machine in cold state) to measure the linear positioning errors of the Matsuura MC.760 VX machining center during the warm-up cycle. The measured travel of the X axis is set to a range of 600 mm with an interval (step) of 1mm and X=0 is selected as the reference point. Linear position errors as well as temperature and air pressure/humidity readings were recorded during the laser measurement cycles. The temperature rise test and error measurement cycles were repeated for a period of 35 h. Data capture is performed by moving the machine (reflector) to several positions (known as "targets") along the axis under test and measuring the machine error. A G-code program was used to move the machine from one position to another according to the available stroke, pausing for a few seconds at each target position. Measurements are taken during each pause along the axis under test. The parameters that must be specified to create the movement program (G code) are:

- the number of runs that the controller will make by the indicated targets;
- the direction of each pass. This can be unidirectional or bidirectional;
- the stopping time at each position before going to the next one;
- an overrun distance, which indicates the region of direction inversion at the end of the axis limit;
- the feedrate to move the movable table from one position to the next.

3 RESULTS AND DISCUSSION

When a machining operation requires great precision, temperature variations can cause errors due to uneven expansion, representing a significant obstacle. These effects can be grouped into three main categories:

- Errors due to overheating of the machine or some of its parts.
- Errors due to changes in ambient temperature and which result from the fact that the thermal inertia of the machine and that of the part are not equal.
- Errors resulting from heating of the part during machining.

Machine heating is often caused by the tool spindle drive motor, which is however not involved in the tests in question. Only the motor that controls the movement of the table is used for these tests, and it is generally less powerful than the spindle motor. To obtain precise machining, it is not necessary for the room temperature to be perfectly stable, but it is crucial that it does not undergo sudden temperature variations. Indeed, the machine has, by its mass, a certain thermal inertia; it does not instantly follow the temperature of the room. It is the same for the part but, as it is much lighter than the machine; its thermal inertia is less. On the other hand, the heat dissipation surface area varies a lot from room to room. This is why the machine must be given the necessary time to follow the variations in the ambient temperature. On the other hand, it is exceptional for a room to have the same temperature on the floor as on the ceiling. This results in errors originating from the temperature gradient having the effect of altering the straightness of the slideways. Finally, it is still very common to see heating devices that cause violent air currents that are harmful to the preservation of the good stability of a precision machine. In this work, the X axis of the Matsuura MC.760 VX CNC machine tool was tested for linear positioning error. Figures 2, 3 and 4 show the variation of air temperature, atmospheric pressure and air humidity during the 36 hours of testing. Figure 2 shows that the air temperature is not perfectly stable during the test, it varies in a range below 2° C. It should be noted, however, that the tests were carried out during the weekend, doors closed workshop spaces and in a non-air-conditioned environment. Figure 2 also shows a linear drift between the 5th and 25th hour, followed by a temperature drop of about 1°C. This temperature drop may be due to the opening of the workshop door by the operator for a verification of the progress of the tests.

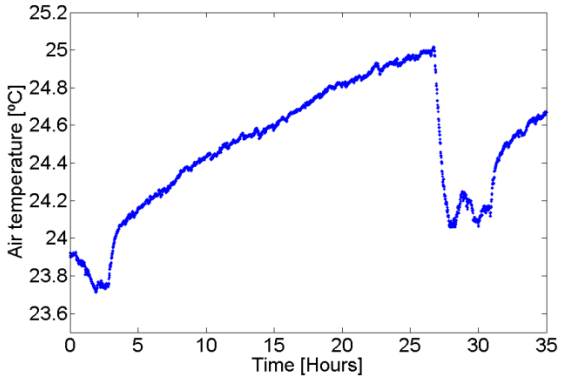

Fig. 2 : Air temperature variation during the test.

On the other hand, Figure 3 shows that the atmospheric pressure increases with time during the first 10 hours to reach a maximum value of 996

mbar and then drops to a minimum value of 992 mbar after 28 hours. Then the atmospheric pressure increases again with time.

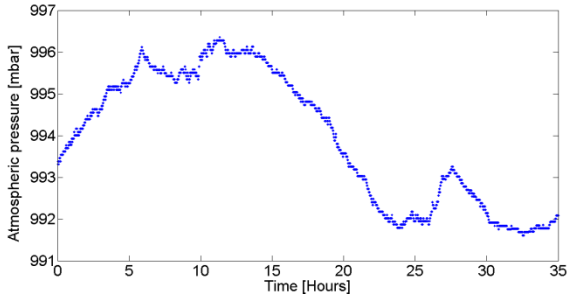

Fig. 3. Variation of atmospheric pressure during the test

Figure 4 shows the variation of air humidity as a function of time. The relative humidity of the air is expressed as a percentage and is defined as the ratio of the quantity of water actually contained in the air and the absorption capacity at a given temperature. Figure 4 also shows that the relative humidity is usually above 49% and varies relatively during the test. The relative humidity during the test oscillate between 49% and 54%.

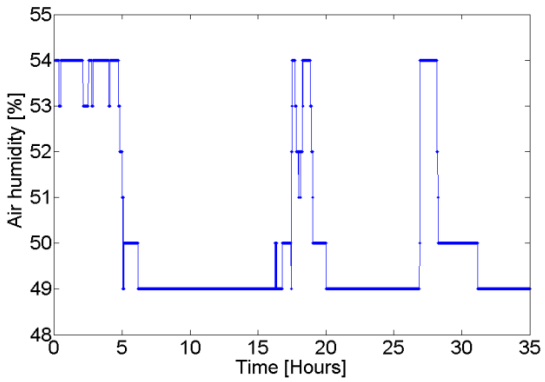

Fig. 4 : Variation of air humidity during the test

Theoretically, the 21 parametric error components (joint kinematic deviations) are all subject to thermal effects. In practice, each machine has its own particular thermal issues depending on its configuration and construction. Therefore, a preliminary study of how the machine structure reacts to rising temperatures is necessary. On the other hand, fluctuations in environmental conditions cause expansion of machine elements and dimensional changes in the part during machining. In addition, the thermal stability of machine tools is essential to ensure the required quality of machined parts. Linear displacement errors along the X axis at different time periods are given in Figure 5. In this figure, the first warm-up cycle indicates that the errors were measured when the machine was cold (0 hours of operation) for forward and backward directions, respectively. The measurement results show that the position errors are generally smaller at the beginning of the axis movement (start position) and have a tendency to increase with the increase of the nominal position of the axis. It was also found that although the linear positioning errors varied with temperature (hour of machine operation), their baseline profiles along the path did not change drastically. The magnitude of the errors gradually increases as the machine warms up.

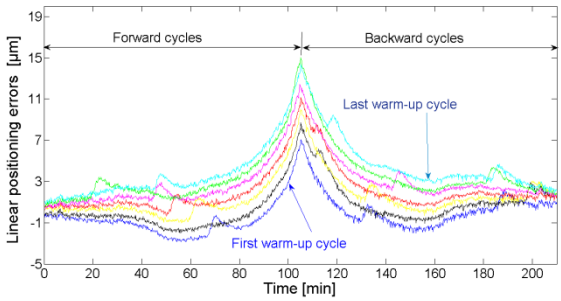

Fig. 5 : Linear positioning errors along the X axis.

It can be clearly seen that each curve has the same variation, but with increasing operating time, the overall change in position deviation becomes larger. After reaching the state of thermal equilibrium, the change gradually slows down and the gap between the curves decreases.

Under cold start conditions, only stationary error profiles (i.e. pure geometric errors) exist in the machine. During the warm-up cycle, time-varying drifts (errors of thermal origin) are added to the geometric errors. When the machine is in the cold state, the maximum linear displacement error is of the order of magnitude of 7 µm. At the end of the warm-up cycle, the error increases to its maximum value of 15 µm.

3.1 Modeling of the thermal effect

Pure geometric errors are considered machine errors, which exist under cold start conditions. During the warm-up cycle, time-varying slopes (thermal errors) are added to the geometric errors.

The empirical model approach, which establishes the relationship between geometric-thermal errors and measured temperatures in conjunction with axis position data, will be used in this work to predict geometric and thermal errors of machine tools. Accordingly, the thermally induced positioning error measured by the laser interferometer can be separated into two parts: one is the static geometric error related to the location of the axis, and the other is the error thermal related to the thermal characteristics and location of the axis. The measured positioning error can be defined as follows:

$$\delta pos = \delta geo + \delta therm \quad (1)$$

Where δpos indicates the measured positioning error of the axis, δgeo is the static geometric error and δtherm is the thermal error.

Thermal gradients produce significant deformations of machine components and consequently additional positioning errors (□therm).

$$\delta therm = p \times \Delta T \times \alpha \quad (2)$$

Where α is the coefficient of thermal expansion (expressed in 10-6/°C) ;

α= 11.7x10-6/°C ;

ΔT is the homogeneous variation of the temperature (°C) ;

p is the length of the tested element (m) ;

Figure 6 shows the predicted thermal error δ_{therm} for the first measurement cycle using the equation (2).

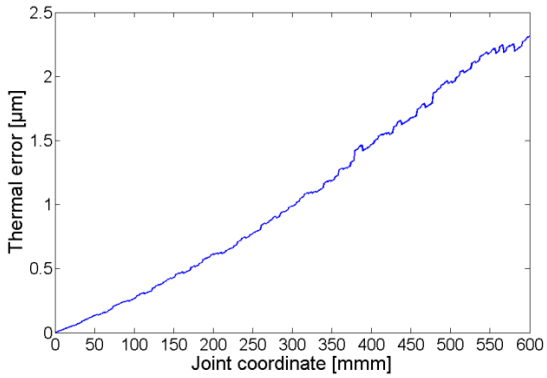

Fig. 6 : Predicted thermal error for the first measurement cycle

Many researchers have studied the method of modeling static geometric errors. Feng [16] proposed a new modeling method based on B-spline curves and achieved high modeling accuracy. Fan [17, 18] proposed the orthogonal polynomials and significantly improved the accuracy of machine tools compared to those without error compensation. Slamani [19] experimentally proved that a polynomial of degree three or four is sufficient to represent the static geometric errors of a MOCN. Based on the results of Slamani [19], a polynomial of degree 3 is adopted in this work to model the static geometric errors.

$$\delta_{geo} = \beta_0 + \beta_1 X + \beta_2 X^2 + \beta_3 X^3 \quad (3)$$

Where, δgeo is the static geometric error (result of the first test (first cycle)) is X is the nominal (programmed) position of the X axis (joint coordinate). According to the equation (1)

$$\delta \text{ geo} = \delta pos - \delta therm \quad (4)$$

equation (3) can be written in matrix form as follows:

$$\begin{bmatrix} \delta_{geo_1} \\ \delta_{geo_2} \\ \vdots \\ \delta_{geo_n} \end{bmatrix} = \begin{bmatrix} 1 & X_1 & X_1^2 & X_1^3 \\ 1 & X_2 & X_2^2 & X_2^3 \\ \vdots & \vdots & \vdots & \vdots \\ 1 & X_n & X_n^2 & X_n^3 \end{bmatrix} \begin{bmatrix} \beta_0 \\ \beta_1 \\ \beta_2 \\ \beta_3 \end{bmatrix} \quad (5)$$

$$\delta = X\beta \quad (6)$$

Equation (6) presents a linear system with four unknowns, the resolution of this equation making it possible to find the coefficients β_i in the sense of least squares. After solving the estimated equation becomes:

$$\delta_{geo} = -0.7579 + 0.0115X + -1.08 \times 10^{-4}X^2 + 1.7 \times 10^{-7}X^3$$

Figure 7 shows that the estimated model is very representative, it offers a quality of adjustment of R^2=90%.

To validate the proposed model, we randomly take a test cycle, say the seventh cycle. For this, the thermal error is predicted again using the equation (2).

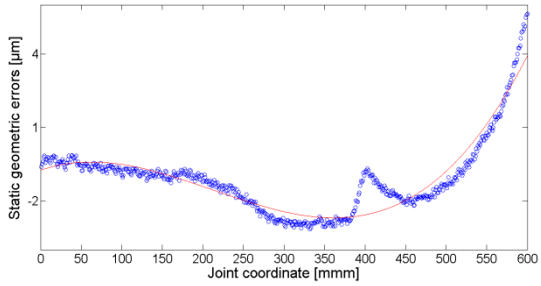

Fig. 7. Measured and predicted positioning error for the first measurement cycle, including thermal effect.

The results obtained are then added to the results of the static geometric errors predicted by the equation (3) and presented in Figure 8.

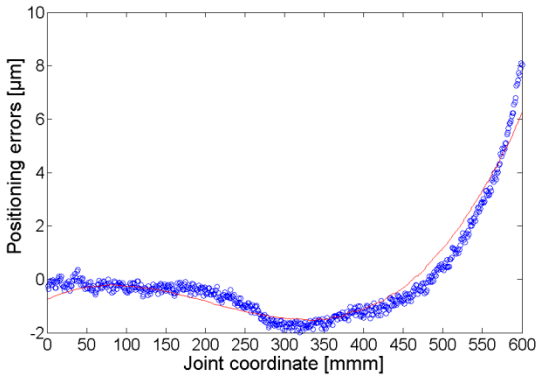

Fig. 8. Measured and predicted positioning error for the seventh measurement cycle, including thermal effect.

A good quality of adjustment ($R^2 = 0.95$) was obtained which proves the validity of the proposed model.

4 CONCLUSION

By focusing on the development of a predictive model for geometric and thermal errors, this study contributed to improving the precision of a machine tool in the machining industry. After analyzing the main sources of errors, the results showed that thermal errors have a great impact. To quantify the thermal behavior of the machine tool, a mathematical model based on the thermal expansion coefficient of the material was used for a homogeneous temperature variation. A geometric errors model is also developed in this paper. The developed geometric error model is integrated with the thermal error model and found to be able to predict the linear positioning error as a function of the position of the slides under different conditions. Although this modeling approach was effective in improving the accuracy of the tested machine tool, the persistent thermal problem in machine tools requires further research to find more effective solutions to minimize its impact.

5 ACKNOWLEDGEMENTS

The authors would like to thank Prof. René Mayer, Yan Boutin and Bu Khanh Vo, for their assistance during the laboratory tests.

6 REFERENCES

1. Zhu, S., Ding, G., Qin, S., Lei, J., Zhuang, L., & Yan, K. (2012). Integrated geometric error modeling, identification and compensation of CNC machine tools. International journal of machine tools and manufacture, 52(1), 24-29.

2. Raksiri, C., & Parnichkun, M. (2004). Geometric and force errors compensation in a 3-axis CNC milling machine. International Journal of Machine Tools and Manufacture, 44(12-13), 1283-1291.

3. Han, Z. Y., Jin, H. Y., Liu, Y. L., & Fu, H. Y. (2013). A review of geometric error modeling and error detection for CNC machine tool. Applied Mechanics and Materials, 303, 627-631.

4. Yang, J., Yuan, J., & Ni, J. (1999). Thermal error mode analysis and robust modeling for error compensation on a CNC turning center. International Journal of Machine Tools and Manufacture, 39(9), 1367-1381.

5. Abdulshahed, A. M., Longstaff, A. P., & Fletcher, S. (2015). The application of ANFIS prediction models for thermal error compensation on CNC machine tools. Applied soft computing, 27, 158-168.

6. Zapłata, J., & Pajor, M. (2019). Piecewise compensation of thermal errors of a ball screw driven CNC axis. Precision Engineering, 60, 160-166.

7. Merghache, S. M., & Hamdi, A. (2020). Numerical evaluation of geometrical errors of three-axes CNC machine tool due to cutting forces—case: milling. The International Journal of Advanced Manufacturing Technology, 111(5-6), 1683-1705.

8. Abas, M., Salah, B., Khalid, Q. S., Hussain, I., Babar, A. R., Nawaz, R., ... & Saleem, W. (2020). Experimental investigation and statistical evaluation of optimized cutting process parameters and cutting conditions to minimize cutting forces and shape deviations in Al6026-T9. Materials, 13(19), 4327.

9. Ramesh, R., Mannan, M. A., & Poo, A. N. (2005). Tracking and contour error control in CNC servo systems. International Journal of Machine Tools and Manufacture, 45(3), 301-326.

10. Andolfatto, L., Lavernhe, S., & Mayer, J. R. R. (2011). Evaluation of servo, geometric and dynamic error sources on five-axis high-speed machine tool. International Journal of Machine Tools and Manufacture, 51(10-11), 787-796.

11. Kim, D. I. (1995, October). Study on interpolation algorithms of CNC machine tools. In IAS'95. Conference Record of the 1995 IEEE Industry Applications Conference Thirtieth IAS Annual Meeting (Vol. 3, pp. 1930-1937). IEEE.

12. Cui, G., Lu, Y., Li, J., Gao, D., & Yao, Y. (2012). Geometric error compensation software system for CNC machine tools based on NC program reconstructing. International Journal of Advanced Manufacturing Technology, 63.

13. Fan, W., Lee, C., Chen, J., & Xiao, Y. (2016). Real-time Bezier interpolation satisfying chord error constraint for CNC tool path. Science China Technological Sciences, 59, 203-213.

14. Yong, T., & Narayanaswami, R. (2003). A parametric interpolator with confined chord errors, acceleration and deceleration for NC machining. Computer-Aided Design, 35(13), 1249-1259.

15. Tsai, M. S., & Huang, Y. C. (2016). A novel integrated dynamic acceleration/deceleration interpolation algorithm for a CNC controller. The International Journal of Advanced Manufacturing Technology, 87(1-4), 279-292.

16. Feng, W. L., Yao, X. D., Azamat, A., & Yang, J. G. (2015). Straightness error compensation for large CNC gantry type milling centers based on

B-spline curves modeling. International Journal of Machine Tools and Manufacture, 88, 165-174.

17. Fan, K., Yang, J., & Yang, L. (2014). Unified error model based spatial error compensation for four types of CNC machining center: part II—unified model based spatial error compensation. Mechanical Systems and Signal Processing, 49(1-2), 63-76.

18. Fan, K., Yang, J., & Yang, L. (2015). Unified error model based spatial error compensation for four types of CNC machining center: part I—singular function based unified error model. Mechanical Systems and Signal Processing, 60, 656-667.

19. Slamani, M., Mayer, J. R. R., & Cloutier, G. M. (2011). Modeling and experimental validation of machine tool motion errors using degree optimized polynomial including motion hysteresis. Experimental Techniques, 35, 37-44.